MATHEMATICAL MODELING AND COMPUTING, Vol. 12, No. 2, pp. 611–620 (2025)

Drying of cappilary-porous materials in an external constant electric field

Gayvas B.[1], Markovych B.[2], Dmytruk V.[2], Dmytruk A.[2], Nagachevska O.[2]

[1] *Pidstryhach Institute for Applied Problems of Mechanics and Mathematics, National Academy of Sciences of Ukraine, 3-b Naukova Str., 79060, Lviv, Ukraine*
[2] *Lviv Polytechnic National University, 12 S. Bandera Str., 79013, Lviv, Ukraine*

(Received 22 February 2025; Revised 13 June 2025; Accepted 15 June 2025)

In the article, the mathematical model for the drying process of a porous layer subjected to an external electric field is developed considering the coupled effects of heat, mass, and charge transport. A system of algebraic equations is obtained to describe the drying dynamics, incorporating key physical parameters such as boundary layer thickness, temperature, and electric field intensity. The model is validated against experimental data, demonstrating its accuracy in predicting moisture distribution over time in a porous materials under the action of constant electric field.

Keywords: *electroosmotic drying; porous materials; moisture removal; capillary effects; heat and mass transfer; electric field intensity; drying kinetics; mathematical modeling; energy-efficient drying; sustainability.*

2010 MSC: 76W05, 80A20, 35Q60, 76S05, 35Q35 **DOI:** 10.23939/mmc2025.02.611

1. Introduction

Drying of porous materials is a critical process in various industrial applications, including food processing, pharmaceuticals, and materials engineering. Traditional drying methods rely primarily on thermal and convective mechanisms, which can be energy-intensive and may cause undesirable changes in material properties. Electroosmotic drying, based on the electrokinetic movement of water under an applied electric field, has emerged as a promising alternative, offering improved drying rates and energy efficiency [1–6]. Techniques that combine this with contact and pulse-based heating are also under active investigation [7].

Electroosmotic drying is an advanced technique that utilizes an external constant electric field to enhance moisture removal from porous materials. This method utilises electrokinetic effects to improve mass transfer efficiency, reducing drying time and energy consumption. Electroosmotic drying is possible due to the presence of a double electric layer at the interface between the pore liquid and the solid matrix. The existence of electrically induced forces alters the dynamics of the drying process.

At the initial stage, a dried zone forms within the body only near a specific part (S_1) of the surface (S), on the side influenced by the applied electric field forces (dried zone 1). The other part of the surface, (S_2), remains wetted. If the electrical force exceeds the capillary force, which is governed by the curvature of the liquid-gas interface, electroosmotic liquid leakage occurs through this region.

As the dried zone expands, its electrical resistance increases, leading to a voltage drop across it. Consequently, the electric field intensity in the liquid-saturated region decreases. The reduction in liquid content during drying also results in a decrease in the total electric charge carried by the liquid. The ponderomotive force $\rho_q \boldsymbol{E}$ (where ρ_q is the average charge density in the diffuse layer and $\boldsymbol{E}$ is the electric field intensity in the pores), which acts on the liquid, diminishes over time. At this stage, the capillary force remains relatively unchanged.

When the electrical and capillary forces reach equilibrium, electroosmotic liquid leakage through the surface (S_2) ceases, and a second dried zone begins to form. From this point forward, the dried regions expand from both (S_1) and (S_2), propagating inward toward each other.

2. Problem statement

Thus, the drying process occurs in two distinct stages: an initial stage characterized by localized electroosmotic liquid migration and a second stage where the dried zones grow deeper into the material, eventually leading to full drying.

First stage of drying. Using the equation of state for a gas mixture and Darcy's law, we derive the Stefan–Maxwell equations for the key variables ρ_a and ρ_v, representing the densities of air and vapor, respectively:

$$\begin{gathered} \rho_a \frac{K_g}{\mu_g} \boldsymbol{\nabla} \left(\frac{\rho_a}{M_a} + \frac{\rho_v}{M_v} \right) RT + D' \boldsymbol{\nabla} \rho_a = 0, \\ \boldsymbol{\nabla} \cdot \left[\rho_v \frac{K_g}{\mu_g} \boldsymbol{\nabla} \left(\frac{\rho_a}{M_a} + \frac{\rho_v}{M_v} \right) RT + D' \boldsymbol{\nabla} \rho_v \right] = 0, \end{gathered} \tag{1}$$

where K_g is the permeability coefficient, dependent on pore radius and shape, μ_g is the dynamic viscosity coefficient of the gas, ρ_a and ρ_v denote the air and vapor densities, M_a and M_v are the molar masses of air and vapor, R is the universal gas constant, T is the absolute temperature, D' is the effective diffusion coefficient.

The equations hold within the region of dried pores, which is bounded by the surfaces S and moving surface S^*. Notably, the system of differential Eqs. (1) exhibits nonlinearity.

On the moving surface S^*, the vapor density can be assumed to equal the saturated vapor density [8]:

$$\rho_v = \rho_{vn}. \tag{2}$$

The boundary conditions at surface S depend on the modeling approach for the interaction between the body and its environment.

In the case of natural drying, where the body is in contact with a mixture of air and vapor, it can be assumed that at a sufficient distance from the surface S, the vapor and air densities, ρ_{ve} and ρ_{ae}, attain constant values corresponding to atmospheric air [8]:

$$\lim_{r \to \infty} \rho_{ve} = \rho_{v1}, \quad \lim_{r \to \infty} \rho_{ae} = \rho_{a1}, \tag{3}$$

where r represents the distance from the surface S.

In the external region relative to the body, mass transfer processes are described by the Stefan–Maxwell equations under the assumption of constant atmospheric pressure:

$$\begin{gathered} \boldsymbol{\nabla} \rho_{ae} - \frac{\rho_{ae}}{D'_e} \boldsymbol{v}_e = 0, \\ \boldsymbol{\nabla} \cdot \left(\boldsymbol{\nabla} \rho_{ve} - \frac{\rho_{ve}}{D'_e} \boldsymbol{v}_e \right) = 0. \end{gathered} \tag{4}$$

Additionally, the gas pressure in the external environment remains constant:

$$P_{ge} = \left(\frac{\rho_{ae}}{M_a} + \frac{\rho_{ve}}{M_v} \right) RT = \text{const}\,. \tag{5}$$

On the surface S, the normal component of vapor flux must be continuous:

$$\boldsymbol{n} \cdot j_v = \left(\boldsymbol{\nabla} \rho_{ve} - \frac{\rho_{ve}}{D'_e} \boldsymbol{v}_e \right) \cdot \boldsymbol{n}, \tag{6}$$

and the component densities must be equal, following from the equality of partial pressures at the surface S:

$$\rho_{ae} = \rho_a, \quad \rho_{ve} = \rho_v. \tag{7}$$

Equations (1)–(7) form a complete system of relations and can be used to describe mass transfer during the natural drying of a porous body.

In studies of drying processes, particularly under intensified blowing conditions, the external problem is often formulated only for a boundary layer of finite thickness δ [9]. In this case, mass transfer in the boundary layer is described by Eqs. (1)–(2). On the surface S of the body, the coupling condition (7) applies, while on the outer surface S^{**} of the boundary layer, the condition is:

$$\rho_{ae} = \rho_{a1}, \quad \rho_{ve} = \rho_{v1}. \tag{8}$$

However, it should be noted that in the first stage, the liquid moves under the influence of electric forces toward the surface (S_2) with velocity:

$$\boldsymbol{v}_L = \frac{K_L}{\mu_L} \left(\rho_q \boldsymbol{E} - \boldsymbol{\nabla} P_k\right),$$

where K_L is the permeability coefficient of the body with respect to the liquid, μ_L is its dynamic viscosity, P_k is the pressure caused by the curvature of the interface between the liquid and gas.

It is assumed that the liquid freely exits the pores. At this stage, phase transition from liquid to vapor near the surface S_2 is not considered. The liquid content in the body decreases both due to drying from surface S_1 and electroosmotic removal through surface S_2. The mass balance equation is given by:

$$\frac{dm}{dt} = -\int_{(S_1)} (j_{v1} \cdot \boldsymbol{n}_1)\, dS_1 - \int_{(S_2)} (j_{v2} \cdot \boldsymbol{n}_2)\, dS_2, \tag{9}$$

where $\boldsymbol{n}_1$ and $\boldsymbol{n}_2$ are the outward normals to surfaces S_1 and S_2; $\boldsymbol{j}_{v1}$ is the vapor flux through surface S_1, obtained solving the problem (1)–(4), or (1), (6), (4)–(8); $\boldsymbol{j}_L$ is the liquid flux through surface S_2.

The liquid flux through surface S_2 is given by:

$$j_L = \Pi \gamma_L \boldsymbol{v}_L.$$

Second stage of drying. At the moment when the electric and capillary forces balance out:

$$\int_{(V_f)} \rho_q\, \boldsymbol{E}\, dV_L - P_k S_1^* = 0, \tag{10}$$

liquid leakage ceases, and a second dried zone forms, expanding inward from surface S_2. In Eq. (10), (V_L) represents the region of the body occupied by liquid; V_L is its volume; S_1^* is the surface area of the gas-liquid interface.

The drying process of zone 2 is formulated similarly to the problem (1)–(7) for zone 1, and the new mass balance equation is:

$$\frac{dm_L}{dt} = -\int_{(S_1)} (j_{v1} \cdot \boldsymbol{n}_1)\, dS_1 - \int_{(S_2)} (j_{v2} \cdot \boldsymbol{n}_2)\, dS_2.$$

Determination of electrical quantities. The electric field intensity is determined from the corresponding electrostatics problems. For the first stage, the governing equation is given as:

$$\Delta\varphi_j = 0, \quad \boldsymbol{E}_j = -\boldsymbol{\nabla}\varphi_j, \quad (j = 1, 2),$$

which applies to the region (V_1) $(j = 1)$, bounded by surfaces (S_1) and (S_1^*), and the region (V_L) $(j = 2)$, occupied by liquid, with the boundary conditions:

$$\varphi_1 = \varphi_{01} \quad \text{on the surface} \quad (S_1), \qquad \varphi_2 = \varphi_{02} \quad \text{on the surface} \quad (S_2),$$

and the conjugation conditions at the interface:

$$\varphi_1 = \varphi_2, \quad \boldsymbol{n}_1 \cdot (\boldsymbol{j}_1 - \boldsymbol{j}_2)_1 = 0 \quad \text{on the surface} \quad (S_1^*),$$

where $\boldsymbol{j}_j = \sigma_j \boldsymbol{E}_j$, $(j = 1, 2)$. Here, $\boldsymbol{j}_1$, $\boldsymbol{j}_2$ are the current density vectors, while σ_1, σ_2 denote the electrical conductivity coefficients in regions (V_1) and (V_L), respectively. The vector $\boldsymbol{n}_1$ represents the normal to the interface (S_1^*).

For the second stage of drying, the electrostatics problem is formulated as:

$$\Delta\varphi_m = 0, \quad \boldsymbol{E}_m = -\boldsymbol{\nabla}\varphi_m, \quad (m = 1, 2, 3),$$

for the regions (V_1) $(m = 1)$, (V_f) $(m = 2)$, and (V_2) $(m = 3)$, bounded by surfaces (S_2^*) and (S_2), under the boundary conditions:

$$\varphi_1 = \varphi_{01} \quad \text{on the surface} \quad (S_1), \qquad \varphi_3 = \varphi_{02} \quad \text{on the surface} \quad (S_2),$$

and the conjugation conditions:

$$\varphi_1 = \varphi_2, \quad \boldsymbol{n}_1 \cdot (\boldsymbol{j}_1 - \boldsymbol{j}_2) = 0 \quad \text{on the surface} \quad (S_1^*),$$
$$\varphi_2 = \varphi_3, \quad \boldsymbol{n}_2 \cdot (\boldsymbol{j}_2 - \boldsymbol{j}_3) = 0 \quad \text{on the surface} \quad (S_2^*),$$

where $\boldsymbol{n}_2$ is the normal to the surface (S_2^*).

The average charge density of the diffuse layer for a binary electrolyte solution, based on the theory of the double electric layer, is determined by the formula:

$$\rho_q = \sqrt{\frac{2\varepsilon_f C\,\Pi}{fRT\,k_p}}\frac{z\,F_f\,\varphi_1}{T_\Gamma},$$

where ε_f is the average absolute dielectric permittivity of the liquid phase, T_Γ is the tortuosity factor, k_p is the permeability coefficient of the porous medium, φ_1 is the surface potential at the closest approach of ions, $z = z_+ = -z_-$, where z_+ and z_- are the valencies of cations and anions, F_f is the Faraday constant, C is the electrolyte concentration, Π is the porosity of the material.

Thus, the problem of electroosmotic drying of a porous body includes the relationships given by Eqs. (1)–(9).

It should also be noted that the use of *an isothermal model* for describing electroosmotic drying requires imposing appropriate restrictions on the magnitude of the external electric field.

3. Electroosmosis drying a layer of capillary-porous material

We consider the problem of the influence of electroosmosis influence on drying a porous layer, where free evaporation occurs on one of its surfaces into the external environment, while the other surface is supplied with moisture from a well-permeable wet medium. This problem can model the drying of basements after floods.

A porous layer initially saturated with moisture is examined, with one of its surfaces (Surface 1) in contact with an environment that is a mixture of air and vapor, while Surface 2 borders a well-permeable wet medium. The air and layer temperatures are assumed to be equal.

Since the vapor in the pores is saturated at the liquid surface, while the surrounding environment is unsaturated, vapor outflow occurs from Surface 1 [10]. As a result, a region of dried pores filled with a mixture of air and vapor is formed within the body, where these components are considered separate constituents of the filling gas. During the drying process, this zone expands deeper into the material. The coordinate of the moving boundary is denoted as $z = L_m$.

To intensify the drying process via electroosmotic moisture removal from the porous layer, a constant potential difference is applied between Surfaces 1 and 2 [11]. Due to the influence of the electric field on the charge of the diffuse part of the electrical double layer at the solid skeleton–pore liquid interface, an additional (ponderomotive) force arises, inducing an electroosmotic moisture flux j_3 toward Surface 2 [12]. Under the action of the electric field, a directed movement of electric charges in the diffuse part of the electrical double layer occurs, accompanied by the movement of the liquid layer along the pore surfaces (electroosmosis).

If a well-permeable wet medium is present on the side of Surface 2, a significant portion of moisture is absorbed into the porous layer through capillary imbibition. Capillary imbibition, driven by the gradient of capillary pressure, results in the formation of a filtration flux j_2.

As a result of the combined action of these fluxes, changes in the relative moisture content of the porous layer occur [13]. Notably, if the dispersion of pore sizes in the porous body model is neglected, the relative moisture content α_m, defined as before, coincides with the phase interface boundary:

$$\bar{z}_m = L_m/L_0.$$

The mass of liquid lost during the drying process is given by:

$$\Delta m = m_{Ln} - m_L = \Pi S \rho_L L_0\,(1 - \bar{z}_m)\,,$$

where S is the pore area, ρ_L is the density of water, and Π is the porosity of the material. Given that the rate of change of liquid mass in the layer is determined by the vapor and liquid flux j from the layer, we arrive at the differential equation governing the relative moisture content α_m in the layer, which can also be interpreted as the equation of motion for the phase interface:

$$\frac{d\alpha_m}{dt} = \frac{d\bar{z}_m}{dt} = -\frac{j(\bar{z}_m)}{\Pi\,\rho_L L_0},$$

where $j(\bar{z}_m)$ is the total flux acting in the porous medium, which is the sum of the vapor flux, the electroosmotic flux, and the flux induced by capillary pressure, counteracting the electroosmotic flow.

The phase transition from liquid to vapor at the gas-liquid interface is accounted for by specifying the density of the saturating vapor on this surface, which depends on the temperature and is given by the formula:

$$\rho_n(T) = 133 \exp\left[18.681 - \frac{4105}{(T-35)}\right] \frac{M_v}{RT} \quad (\mathrm{kg/m^3}).$$

As a result of solving the nonlinear boundary problem, the dependence of the convective-diffusive vapor flux on the parameters of the porous and boundary layers is determined in the form:

$$j_1(\bar{z}_m) = \frac{\Omega}{B - \Gamma_0 \bar{z}_m}, \tag{11}$$

where Ω is a parameter characterizing the intensity of moisture transfer, which depends on the physical properties of the medium and the drying conditions; B is a coefficient that depends on the effective diffusion and permeability characteristics of the porous medium; Γ_0 is a parameter characterizing the influence of the electric field on the mass transfer process.

3.1. Capillary moisture flow

The transfer caused by capillary imbibition is considered. The capillary pressure is determined by the Laplace equation:

$$P_k = P_L - P_g = \frac{-2\sigma_{Lg}\cos\theta}{\bar{R}},$$

where θ is the angle formed by the meniscus surface with the solid surface, P_L and P_g are the pressures in the liquid and gas phases, respectively, σ_{Lg} is the surface tension coefficient at the liquid-gas interface [14].

In the Laplace equation, $\bar{R}$ represents the equivalent Kelvin radius. The flux j_2 caused by capillary imbibition is determined using Poiseuille's equation [15]:

$$j_2 = \Pi \rho_L \frac{K_L}{\mu_L} \frac{P_K}{L_0 \bar{z}_m}, \tag{12}$$

where K_L is the permeability of the liquid, μ_L is the dynamic viscosity of the liquid.

3.2. Electroosmotic moisture flow

The liquid flow caused by the action of an external constant electric field is considered under the condition of the presence of a dried pore zone. The effect of the electric field on the pore liquid is associated with the presence of a double electric layer near the pore surface. The skeleton material is assumed to be hydrophilic, and the minimum transverse pore size is significantly larger than the thickness of the diffuse part of the double electric layer $\delta_e = 1/K_e$, where for a symmetric binary electrolyte solution:

$$K_e = \sqrt{2\pi F_f^2 Z^2 C_0 / \varepsilon^{(1)} RT},$$

where F_f is Faraday's constant, Z is valence of ions considering their charge sign, C_0 is electrolyte solution concentration, $\varepsilon^{(1)}$ is absolute dielectric permeability of the liquid.

Then, on average, the charge density ρ_e in the diffuse part of the double electric layer is determined as:

$$\rho_e = \rho_{e0}\, e^{-K_e(\bar{R}-r)},$$

where ρ_{e0} is charge density value on the surface of capillaries, r is running radial coordinate.

For the assumed condition of the smallness of the double electric layer thickness compared to the capillary radius, $K_e \bar{R} \gg 1$.

The force density across the capillary section:

$$f_e = \rho_e E_L,$$

where $E_L = U_L/L_m$ is electric field intensity, U_L is voltage applied to the liquid-filled part of the capillary.

The average force density:

$$\bar{f}_e = \frac{2\rho_{e0}E_L}{K_e\bar{R}} - \frac{2\rho_{e0}E_L}{(K_e\bar{R})^2}(1 - e^{-K_e\bar{R}}).$$

For the earlier assumption $\bar{R}K_e \gg 1$, we obtain:

$$\bar{f}_e \approx \frac{2\rho_{e0}E_L}{K_e\bar{R}} = \frac{2\bar{\eta}E_L}{\bar{R}},$$

where $\bar{\eta} = \rho_{e0}/K_e$.

The force acting on the charge in the capillary:

$$\bar{F}_e = \bar{f}_e S L_m.$$

The average pressure caused by electrical forces:

$$\bar{P}_e = \bar{F}_e/S = \bar{f}_e L_m.$$

The gradient of this pressure:

$$\boldsymbol{\nabla}\bar{P}_e = \left(d\bar{P}_e/dz\right)\boldsymbol{e}_z, \quad d\bar{P}_e/dz = -\bar{P}_e/L_m = -\bar{F}_e/SL_m = -\bar{f}_e.$$

Considering that the current forces I_g and I_L in the dried and liquid-saturated pore regions are equal, i.e., $I_g = I_L$, according to Ohm's law:

$$I_g = U_g/R_g, \quad I_L = U_L/R_L,$$

we obtain $U_g/U_L = R_g/R_L$. Here: $R_g = \rho_g^*(L_0 - L_m)/S$, $R_L = \rho_L^* L_m/S$, where ρ_g^*, ρ_L^* are the specific resistances of these regions.

As the voltage U between the layer surfaces is $U = U_g + U_L$, then:

$$\frac{U}{U_L} = 1 + \frac{\rho_g^*(1 - \bar{z}_m)}{\rho_L^*\bar{z}_m} = 1 + \frac{(1 - \bar{z}_m)}{\varepsilon_\rho\bar{z}_m}. \tag{13}$$

Here $\varepsilon_\rho = \rho_L^*/\rho_g^*$ is the ratio of specific resistances in the liquid and dried zones, and $\bar{z}_m = L_m/L_0$.

From Eq. (13), it follows that

$$U_L = \varepsilon_\rho U\bar{z}_m/\left[(1 - \bar{z}_m) + \varepsilon_\rho\bar{z}_m\right].$$

Then the electric field intensity in the liquid zone is:

$$E_L = U_L/L_m = \varepsilon_\rho U/L_0\left[(1 - \bar{z}_m) + \varepsilon_\rho\bar{z}_m\right].$$

The formulas for determining the pressure gradient and the magnitude of the electroosmotic flow j_3 are given as follows:

$$\begin{gathered}\frac{d\bar{P}_e}{dz} = -\bar{f}_e = -\frac{2\bar{\eta}}{\bar{R}}\frac{\varepsilon_\rho U}{L_0\left[\varepsilon_\rho\bar{z}_m + (1 - \bar{z}_m)\right]};\\ j_3 = \Pi\rho_L\upsilon_3, \quad \upsilon_3 = \frac{K_L}{\mu_L}\frac{dP_e}{dz} = -\frac{K_L}{\mu_L}\frac{2\bar{\eta}}{\bar{R}}\frac{\varepsilon_\rho U}{L_0\left[\varepsilon_\rho\bar{z}_m + (1 - \bar{z}_m)\right]}.\end{gathered} \tag{14}$$

3.3. Solution of the problem

The determination of the change in relative moisture content during the drying process is reduced to the Cauchy problem [16, 17], where the convective-diffusion flow is determined from Eq. (11), and the capillary and electroosmotic flows are determined from Eqs. (12) and (14), respectively,

$$\begin{gathered}\frac{d\bar{z}_m}{dt} = -\frac{\Omega}{B - \Gamma_0\bar{z}_m} + \frac{\tilde{K}}{\bar{z}_m} + \frac{\tilde{K}_1}{(1 - \bar{z}_m) + K_2\bar{z}_m}, \quad \bar{z}_m(0) = 1;\\ \tilde{K} = \frac{K_L}{\mu_L\bar{R}}\frac{2\sigma_{Lg}}{L_0^2}, \quad \tilde{K}_1 = \frac{K_L}{\mu_L}\frac{2\bar{\eta}\varepsilon_\rho E}{\bar{R}L_0}.\end{gathered} \tag{15}$$

Equation (15) can be written as follows

$$\begin{gathered}\frac{a_{32}\bar{z}_m^3 + a_{22}\bar{z}_m^2 + a_{12}\bar{z}_m}{a_{21}\bar{z}_m^2 + a_{11}\bar{z}_m + a_{01}}\frac{d\bar{z}_m}{dt} = 1;\\ a_{21} = \Omega(1 - K_2) + \tilde{K}\Gamma_0(1 - K_2) - \tilde{K}_1\Gamma_0,\end{gathered}$$

$$a_{11} = -\Omega - \tilde{K}B(1-K_2) - \tilde{K}\Gamma_0 + \tilde{K}_1 B,$$
$$a_{01} = \tilde{K}B, \quad a_{32} = \Gamma_0(1-K_2), \quad a_{22} = -B(1-K_2) - \Gamma_0, \quad a_{12} = B,$$

or

$$\left[\frac{a_{32}}{a_{21}}\frac{\bar{z}_m}{2} + \frac{a_{42}\bar{z}_m^2 + a_{41}\bar{z}_m}{a_{21}\bar{z}_m^2 + a_{11}\bar{z}_m + a_{01}}\right] d\bar{z}_m = dt;$$
$$a_{42} = a_{22} - \frac{a_{32}a_{11}}{a_{21}}, \quad a_{41} = a_{12} - \frac{a_{32}a_{01}}{a_{21}}.$$

The solution of Eq. (15) using the initial condition $\bar{z}_m(0) = 1$ has the form

$$\frac{1}{2}\frac{a_{32}}{a_{21}}\left(\bar{z}_m^2 - 1\right) + \frac{a_{42}}{a_{21}}\left(\bar{z}_m - 1\right) + \left(-\frac{a_{42}a_{11}}{2a_{21}^2} + \frac{a_{41}}{2a_{21}}\right)\ln\left|f_2\left(\bar{z}_m\right)\right| + f\left(\bar{z}_m\right) = t,$$

where

$$f(\bar{z}_m) = \left(\frac{a_{42}(a_{11}^2 - 2a_{21}a_{01})}{2a_{21}^2} - \frac{a_{41}a_{11}}{2a_{21}}\right) f_1(\bar{z}_m),$$

$$f_1(\bar{z}_m) = \frac{2}{\sqrt{4a_{21}a_{01} - a_{11}^2}}\left(\arctan\frac{2a_{21}\bar{z}_m + a_{11}}{\sqrt{4a_{21}a_{01} - a_{11}^2}} - \arctan\frac{2a_{21} + a_{11}}{\sqrt{4a_{21}a_{01} - a_{11}^2}}\right),$$

$$|f_2(\bar{z}_m)| = \left|\frac{a_{21}\bar{z}_m^2 + a_{11}\bar{z}_m + a_{01}}{a_{21} + a_{11} + a_{01}}\right|,$$

if $4a_{21}a_{01} > a_{11}^2$. Otherwise,

$$f_1(\bar{z}_m) = \frac{1}{\sqrt{a_{11}^2 - 4a_{21}a_{01}}}\ln\left|f_3(\bar{z}_m)\right|,$$

where if $a_{11}^2 > 4a_{21}a_{01}$.

In the following section, a numerical analysis of the drying process in a porous layer of cement stone, considering the effects of an external constant electric field, is carried out.

3.4. Results and discussion

Based on the formulas obtained in the previous section, a quantitative analysis of the influence of geometric and physical parameters on the drying a porous layer of cement stone is carried out.

Table 1. Consideration of Capillary Imbibition ($t = 10^4$ s, $L_0 = 0.1$ m).

	δ	$T_1 = 300$ K	$T_2 = 310$ K	$T_3 = 320$ K	$T_4 = 330$ K
$\alpha_m = \bar{z}_m$	0.0001	0.573	0.428	0.254	0.082
	0.001	0.591	0.445	0.27	0.091
	0.01	0.727	0.59	0.416	0.209
	0.1	0.967	0.933	0.875	0.784

Table 1 shows the dependence of relative moisture content at a fixed point in time on temperature and boundary layer thickness during capillary infiltration under natural drying (without an electric field). The influence of an external constant electric field is illustrated by the data given in Tables 2 and 3 for different boundary layer thicknesses.

Table 2. Influence of Electric Field Intensity on Relative Moisture Content at $E = 200$ V/m.

	δ (m)	$T_1 = 300$ K	$T_2 = 310$ K	$T_3 = 320$ K	$T_4 = 330$ K
$\alpha_m = \bar{z}_m$	0.0001	0.561	0.415	0.242	0.075
	0.001	0.577	0.432	0.257	0.083
	0.01	0.705	0.569	0.396	0.193
	0.1	0.914	0.873	0.81	0.718

In Figures 1 and 2, the dynamics of relative moisture content dependence on time is shown for $\delta = 0.001$ m and $\delta = 0.1$ m, respectively, for $T = 300$ K, 310 K, 320 K, and 330 K.

From the provided quantitative data, it follows that the intensity of drying significantly depends on the thickness of the boundary layer. When the thickness of the boundary layer increases by a factor of

100, the relative moisture content increases by a factor of 10 or more. At a boundary layer thickness of $\delta = 0.1$ m and temperatures of 300 K, 310 K, and 320 K, the relative moisture content decreases by no more than 10% over approximately 3 hours.

Table 3. Influence of Electric Field Intensity on Relative Moisture Content at $E = 400$ V/m.

	δ (m)	$T_1 = 300$ K	$T_2 = 310$ K	$T_3 = 320$ K	$T_4 = 330$ K
$\alpha_m = \bar{z}_m$	10^{-4}	0.524	0.377	0.206	0.059
	10^{-2}	0.647	0.511	0.343	0.149

An electric field intensity of $E = 200$ V/m and $E = 400$ V/m (these are not high fields) counteracts liquid infiltration through wall 2, leading to a resultant reduction in relative moisture content of up to 40%.

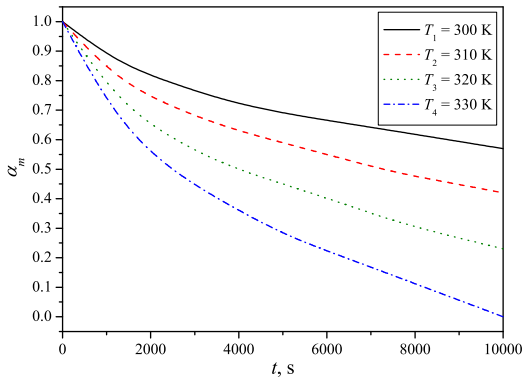

Fig. 1. Dependence of relative moisture content on time at different temperatures for $\delta = 0.001$ m.

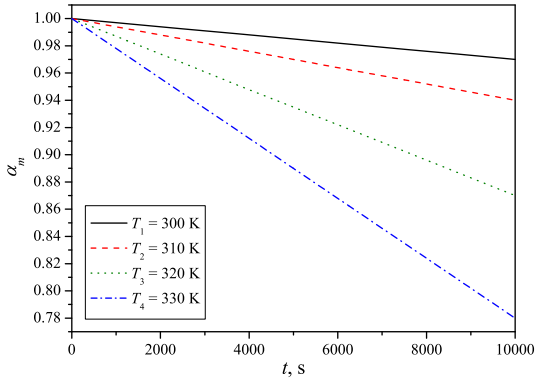

Fig. 2. Dependence of relative moisture content on time at different temperatures for $\delta = 0.1$ m.

One of the primary findings is the strong dependence of drying intensity on the thickness of the boundary layer. As shown in Table 1, increasing the boundary layer thickness by a factor of 100 can lead to a tenfold increase in relative moisture content. This indicates that a thicker boundary layer significantly slows the drying process by impeding moisture transport. At a boundary layer thickness of $\delta = 0.1$ m, the reduction in moisture content over approximately three hours does not exceed 10% at temperatures of 300 K, 310 K, and 320 K. These findings emphasize the importance of controlling the boundary layer characteristics to optimize drying rates.

The role of temperature in accelerating the drying process is evident from Figures 1 and 2. Higher temperatures enhance drying efficiency by increasing vapor pressure gradients and molecular diffusion. The relative moisture content at the final stage of drying is significantly lower at $T = 330$ K compared to $T = 300$ K for all considered boundary layer thicknesses. This confirms that temperature is a critical parameter in determining the speed of moisture removal, with higher temperatures leading to more efficient drying.

The introduction of an external electric field has been shown to affect the drying dynamics significantly. The data presented in Tables 2 and 3 demonstrate that applying an electric field intensity of $E = 200$ V/m.

The numerical modeling results indicate that electroosmotic drying offers significant advantages over both convective and natural drying methods. Specifically, applying an electric field intensity of 200 V/m and 400 V/m effectively enhances moisture removal by reducing capillary-held liquid, leading to a fourfold decrease in relative moisture content compared to convective drying experiments conducted over the same time period [18–22].

4. Conclusions

The findings reveal the significant influence of geometric and physical parameters on drying kinetics. A key observation is that increasing the boundary layer thickness significantly slows drying, while higher temperatures accelerate moisture removal. Applying an electric field intensity of 200 V/m and

400 V/m effectively reduces capillary-held liquid, leading to a decrease in relative moisture content by approximately 40%. This confirms that electroosmotic drying enhances drying efficiency, particularly for cementitious and other porous materials where capillary drying alone is insufficient.

From a practical perspective, the results indicate that electroosmotic drying offers a promising alternative to conventional drying methods, providing a more energy-efficient solution for industrial applications. Future research should explore the combined effects of alternating electric fields and different frequencies to optimize drying performance further while minimizing energy consumption. This study establishes a strong foundation for developing advanced drying technologies based on electrokinetic principles.

[1] Wang C., Kou X., Zhou X., Li R., Wang S. Effects of layer arrangement on heating uniformity and product quality after hot air-assisted radio frequency drying of carrot. Innovative Food Science & Emerging Technologies. **69**, 102667 (2021).

[2] Mutukuri T. T., Darwish A., Strongrich A. D., Peroulis D., Alexeenko A., Zhou Q. Radio frequency – assisted ultrasonic spray freeze drying for pharmaceutical protein solids. Journal of Pharmaceutical Sciences. **112** (1), 40–50 (2023).

[3] Huang D., Yang P., Tang X., Luo L., Sunden B. Application of infrared radiation in the drying of food products. Trends in Food Science & Technology. **110**, 765–777 (2021).

[4] Pawar S. B., Pratape V. M. Fundamentals of infrared heating and its application in drying of food materials: A review. Journal of Food Process Engineering. **40** (1), e12308 (2017).

[5] Awuah G. Radio-Frequency Heating in Food Processing: Principles and Applications. Boca Raton, CRC Press (2014).

[6] Metaxas A. C. Foundations of Electroheat: A Unified Approach. John Wiley & Sons (1996).

[7] Dmytruk V., Gayvas B., Kaminska O., Pastyrska I., Dmytruk A., Nezgoda S. Simulation of Crack Resistance of Mustard in Pulsed Drying Mode. International Scientific and Technical Conference on Computer Sciences and Information Technologies. 91–94 (2020).

[8] Fridrisberg D. A. Course of colloidal chemistry. Khimiya (1984).

[9] Romanenko P. N. Heat and mass transfer and friction in gradient flow of liquids. Energiya (1971).

[10] Melada J., Gargano M., Veronese I., Ludwig N. Does electro-osmosis work in moisture damage prevention? Applicability of infrared-based methods to verify water distribution under electric fields. Journal of Cultural Heritage. **31** (Suppl.), S38–S45 (2018).

[11] Ivliev E. A. Electroosmotic drying of building walls and basements. Surface Engineering and Applied Electrochemistry. **43**, 291-–296 (2007).

[12] Li H., Ottosen L.M. Dewatering and valorizing lake sediments by electroosmotic dewatering for lakes restoration. Environmental Science and Pollution Research (2024).

[13] Gao Y., Wang C., Gong Z., Li Z. A mini review on electroosmotic phenomena in porous media. Energy Storage and Conversion. **2** (3), 480 (2024).

[14] Jin H., Zhang L., Wang B., Fang C., Wang L. Effects of electrode materials and potential gradient on electro-osmotic consolidation for marine clayey soils. Frontiers in Earth Science. **12**, 1260045 (2024).

[15] Thanh L. D., Sprik R., Do P., Nghia N., Nga P. Drying of fluid saturated porous materials by electroosmosis. Current Applied Science and Technology. **21** (1), 26–35 (2021).

[16] Sokolovskyy Y., Drozd K., Samotii T., Boretska I. Fractional-order modeling of heat and moisture transfer in anisotropic materials using a physics-informed neural network. Materials. **17** (19), 4753 (2024).

[17] Decker Ž., Tretjakovas J., Drozd K., Rudzinskas V., Walczak M., Kilikevičius A., Matijosius J., Boretska I. Material's strength analysis of the coupling node of axle of the truck trailer. Materials. **16** (9), 3399 (2023).

[18] Gayvas B. I., Dmytruk V. A. Investigation of drying the porous wood of a cylindrical shape. Mathematical Modeling and Computing. **9** (2), 399–415 (2022).

[19] Gayvas B., Dmytruk V., Semerak M., Rymar T. Solving Stefan's linear problem for drying cylindrical timber under quasi-averaged formulation. Mathematical Modeling and Computing. **8** (2), 150–156 (2021).

[20] Gayvas B., Markovych B., Dmytruk A., Havran M., Dmytruk V. The methods of optimization and regulation of the convective drying process of materials in drying installations. Mathematical Modeling and Computing. **11** (2), 546–554 (2024).

[21] Dmytruk A. Modeling mass transfer processes in multicomponent capillary-porous bodies under mixed boundary conditions. Mathematical Modeling and Computing. **11** (4), 978–986 (2024).

[22] Gayvas B. I., Markovych B. M., Dmytruk A. A., Dmytruk V. A., Havran M. Numerical modeling of heat and mass transfer processes in a capillary-porous body during contact drying. Mathematical Modeling and Computing. **10** (2), 387–399 (2023).

Сушіння капілярно-пористих матеріалів у зовнішньому постійному електричному полі

Гайвась Б.[1], Маркович Б.[2], Дмитрук В.[2], Дмитрук А.[2], Нагачевська О.[2]

[1] *Інститут прикладних проблем механіки та математики ім. Я. С. Підстригача, Національна академія наук України, вул. Наукова, 3б, 79060, Львів, Україна*
[2] *Національний університет "Львівська політехніка", вул. С. Бандери, 12, 79013, Львів, Україна*

У статті розроблено математичну модель процесу сушіння пористого шару під впливом зовнішнього електричного поля з урахуванням зв'язаних ефектів переносу тепла, маси та заряду. Отримано систему алгебраїчних рівнянь для опису динаміки сушіння, що включає ключові фізичні параметри, такі як товщина граничного шару, температура та інтенсивність електричного поля. Модель підтверджено експериментальними даними, що демонструє її точність у прогнозуванні розподілу вологи з часом в шарі пористого матеріалу під дією зовнішнього електричного поля сталої дії.

Ключові слова: *електроосмотична сушка; пористі матеріали; відведення вологи; капілярні ефекти; тепломасообмін; напруженість електричного поля; кінетика сушіння; математичне моделювання, енергоефективне сушіння, екологічність.*